

Effects of Carbon Black on the Electrochemical Performance of Lithium-Organic Coordination Compound Batteries

Peng Bu, Suqin Liu*, Yuan Lu, Shuxin Zhuang, Haiyan Wang, Feiyue Tu

College of Chemistry and Chemical Engineering, Central South University, Changsha 410083, China

*E-mail: sqliu2003@126.com

Received: 13 March 2012 / Accepted: 3 April 2012 / Published: 1 May 2012

Anthraquinone has been proposed as a promising positive electrode material for lithium-organic coordination compound batteries. The electrochemical performances of the organic radical batteries with traditional electrolyte-LiPF₆ are evaluated by different content of carbon black. The cell with 40% of carbon black additive shows superior conductivity and electrochemical properties including higher discharge capacity, better cycle performance, decreased electrochemical impedance spectra compared with the conventional amount of 10% carbon black. When the content is up to 50%, the electrochemical performances are declining a little than 40%, but still higher than 10%. Adding up to 80% amount of electrical conductivity, the cell shows a dramatic drop in all the electrochemical performance.

Keywords: Lithium-organic coordination compound; Carbon black; Anthraquinone; Li-ion batteries

1. INTRODUCTION

In order to power our modern and future life, researchers have made a lot of efforts to find new cathode materials to build better rechargeable lithium batteries [1]. This will not only raise concerns about the finite quantity of some resources on the earth and its environmental intolerance but also about overall CO₂ management [2]. The conventional cathode materials of Li-ion batteries (e.g. LiCoO₂, LiNiO₂) are obtained from limited mineral resources and synthesized by high temperature reactions. Furthermore, safety issues in lithium metal oxide cathodes are critical because of their intrinsic thermal properties. To overcome such problems efficiently, Armand, Chen, and co-workers [2–6] recently have proposed a new class of sustainable lithium batteries based on organic compounds with higher safety, higher capacity and richer reserves in nature.

Compared with the conventional inorganic materials, the organic compounds as cathode materials for lithium batteries have the advantages of higher theoretical specific capacity, abundance of

raw materials, environmental friendliness, feasible structure designability and system safety. Herein, we are interested in organic compound quinones, whose electrochemical behavior has been described in numerous papers [7–10]. The previous investigation shows that quinone has good redox performance and electrochemical reversibility. Furthermore, some of the quinones can eventually be extracted directly from biomass [2,3]. Therefore, quinones compounds are promising energy storage materials [4]. However, the fact should not be ignored that quinones materials have several disadvantages (low electrical conductivity and solubility in electrolytes) [11]. It was confirmed that turning quinones into polymers was an effective method to address the dissolving problem [11-16], and Zhao[17] have tried “parasiting” quinone into a self-prepared mesoporous carbon to improve the electrical conductivity of quinone, but preparing the composite was complicated and needed high temperature and high pressure.

Herein, we focus our attention on 9, 10-anthraquinone (referred as AQ in the following text), which is a cheap industrial raw material and has a high theoretical specific capacity of 257 mAh/g. To overcome the poor electrical conductivity, AQ will be incorporated with a large amount of carbon black in the electrode. Meanwhile, increasing conductive material can also increase the utilization of active material and lower the internal resistance of the cathode [17]. In this work, we prepared four composites with various different ratios of carbon black and investigated their electrochemical performance.

2. EXPERIMENTAL

Conductive carbon blacks (Super P) were provided by Timcal Graphite & Carbon. Anthraquinone (AQ) was purchased by Sigma-Aldrich Company(97%) and used without further purification.

A JSM-6360LV scanning electron microscope (SEM) was used to characterize the morphology and size of the products. Infrared spectra were obtained by a Nicolet 6700 Fourier transform infrared spectrophotometer, using KBr pellets in the 4000-400 cm^{-1} region with a resolution of 4 cm^{-1} by accumulating 16 scans.

The composites were prepared in the following weight ratios: a) AQ-10 (AQ: Carbon black: PTFE=8:1:1); b) AQ-40 (AQ: Carbon black: PTFE=5:4:1); c) AQ-50 (AQ: Carbon black: PTFE=4:5:1); d) AQ-80 (AQ: Carbon black: PTFE=1:8:1).

CR2016-type coin cells consisted of a radical based cathode and lithium foil anode, and separated by a Celgard 2300 membrane. The electrolyte was 1M LiPF_6 -EC + EMC + DMC ($V_{\text{EC}}: V_{\text{EMC}}: V_{\text{DMC}} = 1 : 1 : 1$). The cells were assembled in an argon-filled MB200B glove box. The cells were galvanostatically charged and discharged in the voltage range from 1.5 to 3.0V versus Li/Li^+ . Cyclic voltammogram measurements were performed on CHI660C electrochemical working station at scanning rate of 0.1 mV/s (Shanghai, China). All the electrochemical tests were performed at room temperature.

3. RESULTS AND DISCUSSION

The Anthraquinone crystals were first characterized by scanning electron microscopy (SEM). Figure 1 shows numerous needle-like crystals arranged disorderly. It can be seen that the average diameter of these rods is approximately 1 μm but the length is differ.

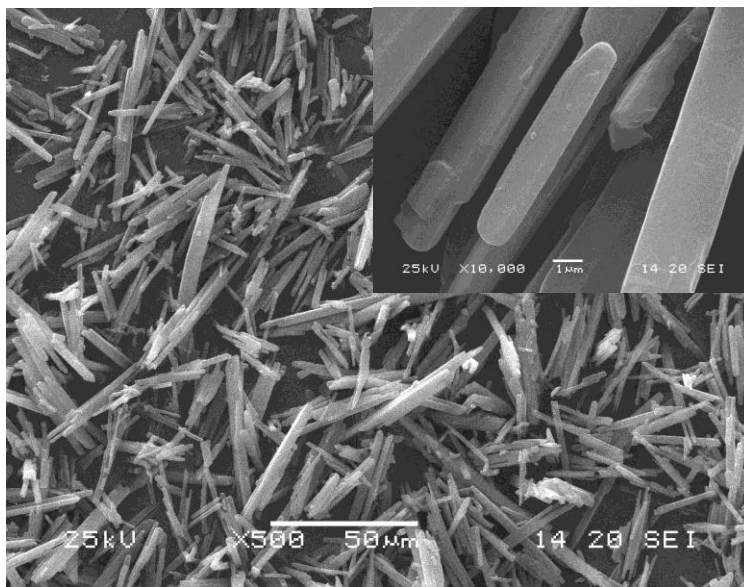


Figure 1. Low and high magnification (inset) SEM images of the Anthraquinone crystals

FTIR spectra of all four composites, i.e. AQ-10, AQ-40, AQ-50 and AQ-80, are shown in Figure 2a and 2b. For comparison, FTIR spectra of carbon black and AQ are also given. As observed, FTIR spectra of AQ and AQ-10 show a strong resemblance in their main characteristic IR bands, while the absorption bands of the compounds become a little broader. In both spectra, the main signal at 1670 cm^{-1} can be ascribed to the stretching of carbonyl group, and four distinct peaks with different intensities from 1450 cm^{-1} to 1600 cm^{-1} are due to quinone skeletal stretching vibrations, respectively. The absorptions at 1592 and 1581 cm^{-1} are assigned to the stretching vibration of the C=C bond in the aromatic ring [17]. Many other similar characteristic bands can be also observed, indicating that the anthraquinonyl group is well maintained after grinding the AQ and carbon black. Unlike that of pure AQ, the spectrum of AQ-40 exhibits a broad peak at 1575 cm^{-1} on the account of adding carbon black. FTIR spectrum of AQ-10 is totally in agreement with AQ, while the spectra of AQ-50, AQ-80, and the pure carbon black are almost the same, the absorption peak of AQ-40 combines the AQ and carbon black at an optimal proportion.

The charge/discharge profiles of the four compounds are based on the current rate of 26 mA/g (about 0.1 C). As shown in Fig. 3a, the charge/discharge curves of AQ-80 are without a noticeable plateau, which is probably due to the active material is too little and the active material distributes unevenly. The particularly inclined region above 2.6 V versus lithium reference probably corresponds

to charging of the carbon black surface. Its capacity is considerably lower than AQ-50, while it contains much more carbon black than others.

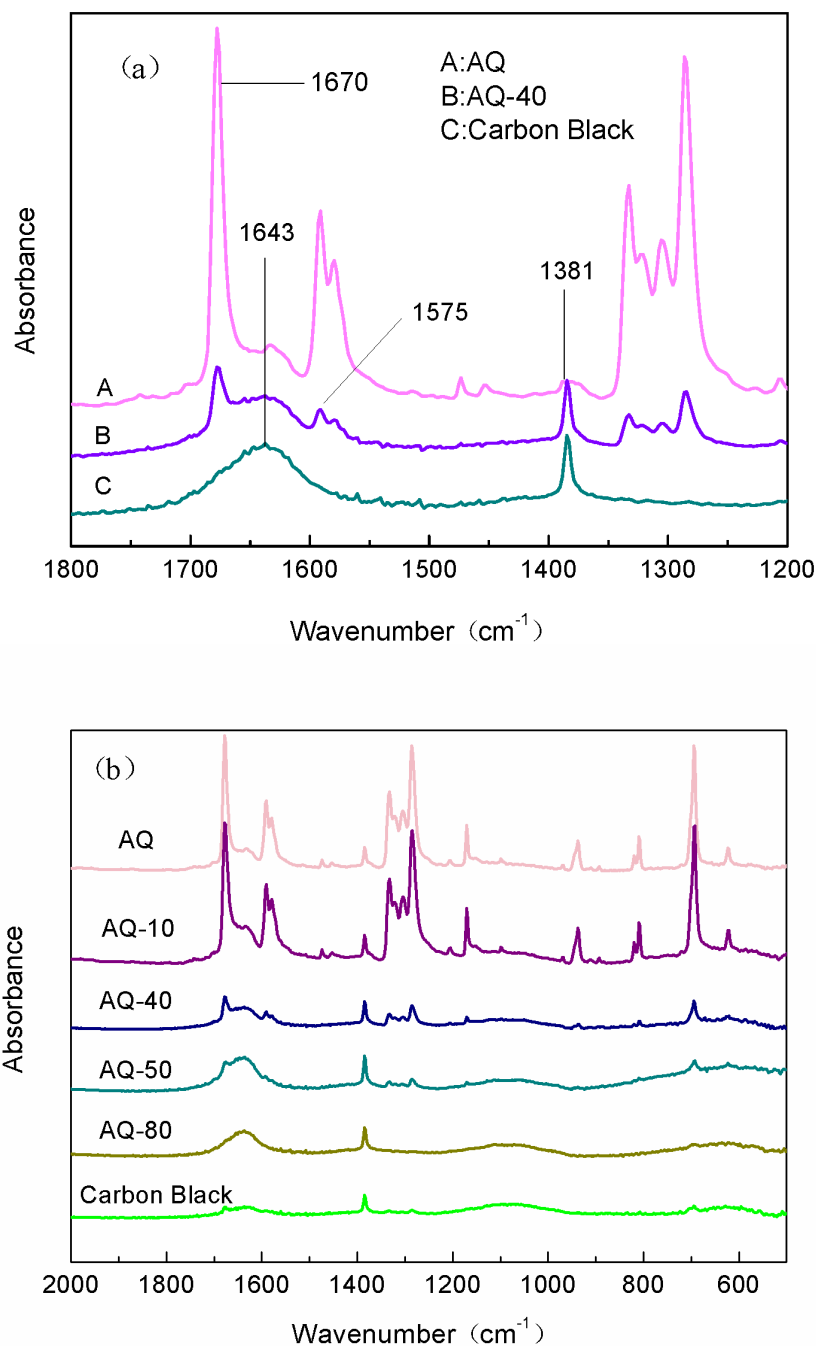


Figure 2. FTIR spectra of AQ, carbon black and the four composites with different amounts of carbon black.

Meanwhile, two distinct voltage plateaus in the discharge process for AQ-40 and AQ-50 are observed at around 2.3 V and 2.1 V, respectively, which are consistent with previous results [13, 14]. The first discharge plateau is about 140 mV higher. But the second discharge plateau of AQ-40 or AQ-

50 is about 100 mV lower than that in AQ-10, which could be explained by the significant difference in conductivity owing to the various carbon black ratios. Similarly, it can be observed that the discharge capacities of AQ-40 and AQ-50 are 212mAh/g and 201mAh/g, respectively, which are much larger than AQ-10. It is ascribed that carbon black owns a larger specific surface area and more edge sites than that of AQ. Increasing carbon black content improves the capacity only at a certain extent. If suitably proportioned, the cathode will exhibit good electrochemical performance (high discharge capacity and high plateau voltage). Obviously, AQ-40 shows the lowest polarization and highest discharge capacity among the four samples, and it is more acceptable for the use as organic cathode material.

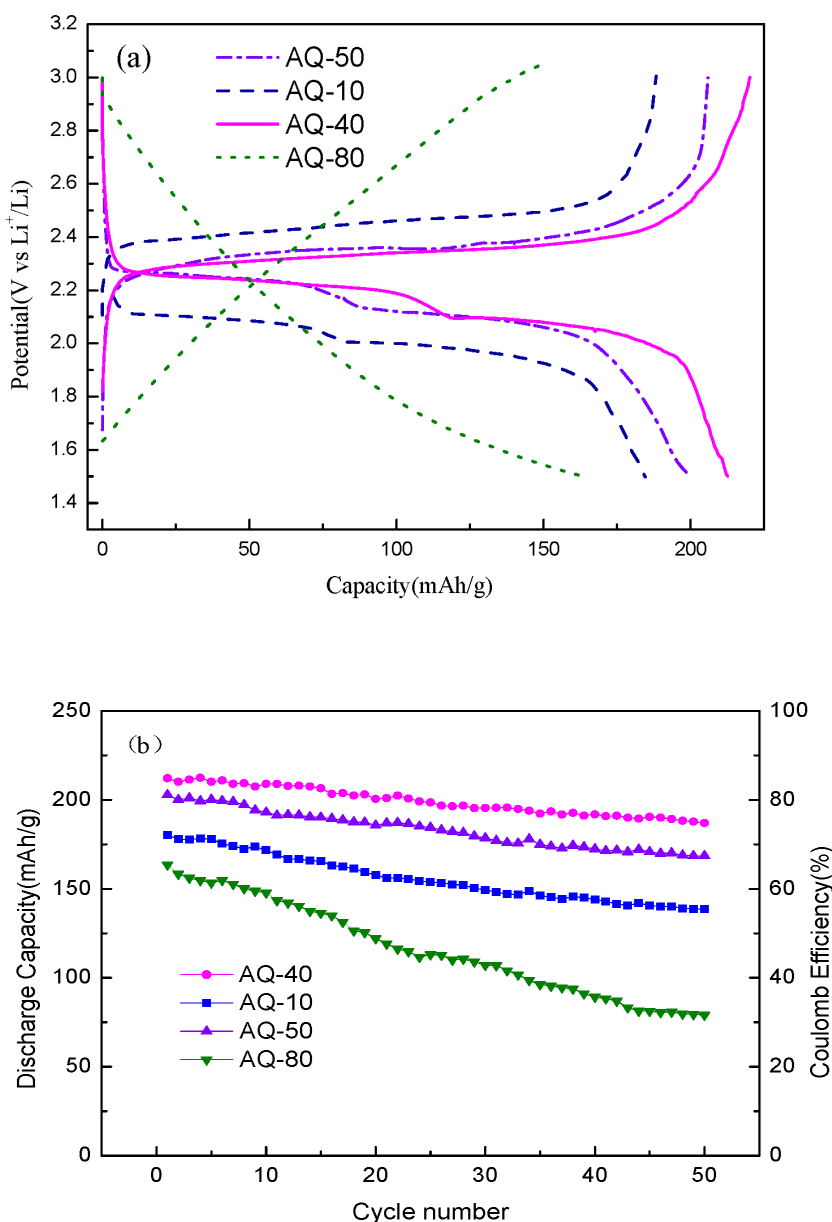


Figure 3. a) Initial charge and discharge curves of the four samples (Charge and discharge rates are both 0.1C, and the voltage range is 1.5-3.0V); b) discharge capacity and coulomb efficiency vs. cycle number for the four samples under 0.1C within 50 cycles.

Cycling performance and associated coulomb efficiency of the four samples at 0.1 C within voltage limits of 1.5-3.0 V are shown in Fig. 3b. In the first cycle of AQ-10, a specific discharge capacity of 181 mAh/g is obtained. However, in subsequent cycles the composite is not very stable. Its capacity loss of the second cycle is 1.6% (3 mAh/g), which may be due to the irreversibility of the SEI layer. After 50 cycles, the coulomb efficiency is 53%, which is still unsatisfactory. Note that the electrode of AQ-40 retained 84% coulomb efficiency of the initial capacity after 50 cycles. The initial discharge capacity is 212 mAh/g, about 82.5% of its theoretical value (257 mAh/g). When the content of carbon black exceeds recommended dosage, especially over the ratio of 40% in the mixture, the discharge capacity fading is increased. The improved cycle performance is partly attributed to the fact that increasing the carbon black ratio could improve the conductivity, as well as the receptivity electricity of the cathode [18], thus raise the discharge capacity and the coulomb efficiency.

Fig. 4a shows the cyclic voltammetry (CV) of the three samples (AQ-10, AQ-40, AQ-50) at a scan rate of 0.1mV/s. The CV curve of AQ-40 shows a pair of well-forming redox peaks centering at 2.2 V, and the peak separation is only 0.2 V. It means that a small polarization is involved in the redox process, which is consistent with the charge/discharge curves. AQ-10 has a peak separation of 0.5 V, which redox peaks become broad and somewhat split. Additionally, the anodic peaks shift to more negative potential and the cathodic peaks shift to more positive potential. These results indicate that the AQ-40 has a smaller polarization than AQ-80. While the redox peaks of AQ-50 center at 2.2 V and its separation remains 0.33 V, just like the AQ-40. The slight variation in the voltammetry of AQ-40 and AQ-50 may be explained by their slightly different content of carbon black.

The redox mechanism in Fig. 4b and 4c reveals that the electrochemical reduction of anthraquinonyl group is unlike the conventional lithium secondary battery. Firstly, the radical anion (AQ[•]) is generated and then the dianion (AQ²⁻) is formed, accompanied by Li⁺ association. In the re-oxidation process, carbonyl groups are rebuilt and Li⁺ is re-ejected into the electrolyte. Based on this concept, two pairs of redox peaks should be found in the observed CV curves. However, from the CV curves shown in Fig. 4a, two anodic peaks and one cathodic peak. Utilizing C=O bearing organic molecules that react with Li, the two-step progresses is separated by a ΔV . Since each ΔV is based on the respective potential values of each process, these can be tuned by chemical modification (e.g., by changing the active materials, substituting functional groups, or adding heteroatoms), so as to either separate or merge the two redox processes [5].

Fig. 5 shows electrochemical impedance spectra of four samples and the equivalent circuit (inset). The real-axis intercept at the high frequency region corresponds to the electrolyte resistance (R_s) and the semicircle at low frequency region corresponds to the electrode/electrolyte interface resistance (R_1) [19]. From the intercept of the semicircle on X axis, the values of R_s are similar for the AQ-10 to AQ-50.

When comparing the diameters of the semicircle appearing in the higher frequency region, AQ-40 showed smaller diameter, indicating the lower resistance of charge transfer reaction than that with AQ-10. The value of R_1 in AQ-80 is the biggest of the four samples, which is ascribed to the fact that the conductive material is swollen by electrolyte, resulting in the increasing of the surface area contacting the electrolyte [20]. Thus the electrode with AQ-40 demonstrated lower charge transfer resistance than that of AQ-10.

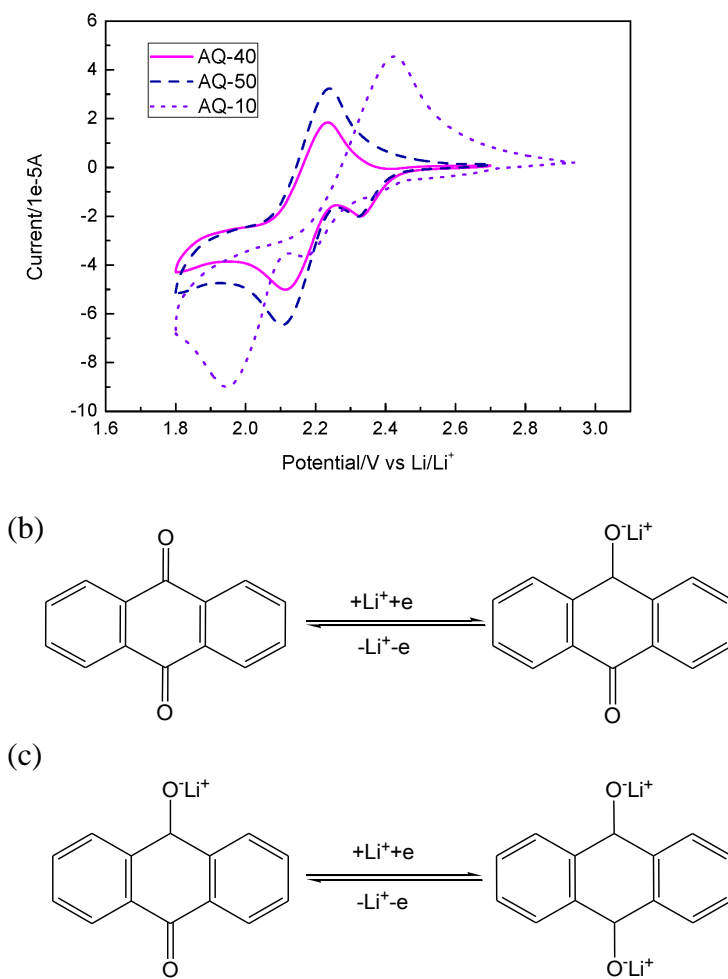


Figure 4. a) Cyclic voltammogram curves of the three samples (AQ-10, AQ-40, AQ-50), scan rate: 0.1mV/s; b) and c) Scheme of redox mechanism of AQ.

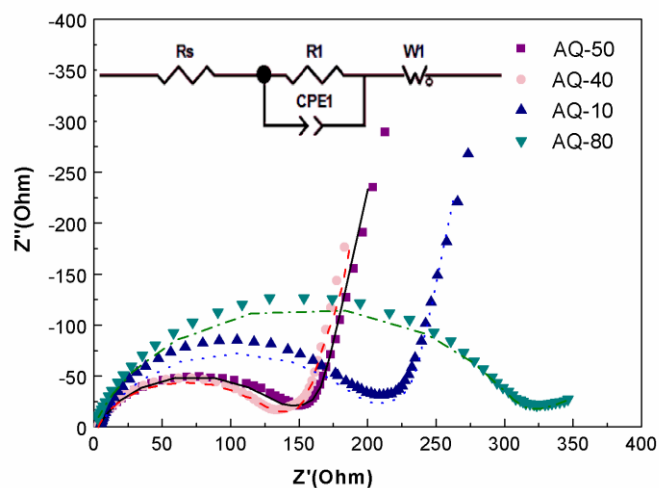


Figure 5. Electrochemical impedance spectra of the four samples and the equivalent circuit (inset).

4. CONCLUSIONS

Conducting agents play significant roles in the electrochemical performance of lithium-organic coordination compound batteries. Adding an optimum content of carbon black is considered as one of the strategies to improve the low electronic conductivity and solubility in traditional electrolytes: $\text{LiPF}_6\text{-EC} + \text{EMC} + \text{DMC}$ ($V_{\text{EC}}: V_{\text{EMC}}: V_{\text{DMC}} = 1 : 1 : 1$). In contrast, AQ-40 ensures the efficient electronic transport throughout the cathode, which endows higher reversible capacity, better cycling stability and decreased the interface resistance than AQ-10, AQ-50 and AQ-80, when carbon black is used as conductive additives for lithium-organic coordination compound batteries. 40% amount of carbon black is expected to become a promising ratio of carbon black as conductive additives for a new class of sustainable lithium batteries based on organic compounds in future.

ACKNOWLEDGEMENTS

This work was financially supported by Chinese 863 program (No. 2008AA031205).

References

1. M.S. Whittingham, *Chem. Rev.* 104 (2004) 4271.
2. M. Armand, S. Grugeon, H. Vezin, S. Laruelle, P. Ribière, P. Poizot, J.-M. Tarascon, *Nat. Mater.* 8 (2009) 120.
3. H.Y. Chen, M. Armand, G. Demailly, F. Dolhem, P. Poizot, J. -M.Tarascon, *ChemSusChem* 1 (2008) 348.
4. W. Walker, S. Grugeon, O. Mentré, S. Laruelle, P. Ribière, J. M. Tarascon, F. Wudl, *J. Am. Chem. Soc.* 132 (2010) 6517.
5. H.Y. Chen, M. Armand, M. Courty, M. Jiang, C. P. Grey, F. Dolhem, J.-M. Tarascon, P. Poizot, *J. Am. Chem. Soc.* 131 (2009) 8984.
6. H.Y. Chen, M. Armand, M. Courty, M. Jiang, C. P. Grey, F. Dolhem, J. M. Tarascon, P. Poizot, *Electrochem. Solid-State Lett.* 12 (2009) A102.
7. M.C.E. Bandeira, G. Maia, *Electrochim. Acta*, 53 (2008) 4512.
8. P. Tissot, A. Huissoud, *Electrochim. Acta*, 41 (1996) 2451.
9. L. Jectic, G. Manning, *J. Electroanal. Chem.* 26 (1970) 195.
10. H. Alt, H. Binder, A. Kohling, G. Sandstede, *Electrochim. Acta*, 17 (1972) 873.
11. Z.P. Song, H. Zhan, Y.H. Zhou, *Chem. Commun.* (Cambridge), 4 (2009) 448.
12. J.F. Xiang, C.X. Chang, M. Li, S.M. Wu, L.J. Yuan, and J.T. Sun, *Cryst. Growth Des.* 8 (2008) 280.
13. Z.P. Song, H. Zhan, and Y.H. Zhou, *Angew. Chem. Int. Ed.* 49 (2010) 8444.
14. T.L. Gall, K.H. Reiman, M.C. Grossel, J.R. Owen, *J. Power Sources*, 119 (2003) 316.
15. L.J. Xue, J.X. Li, S.Q. Hu, M.X. Zhang, Y.H. Zhou, C.M. Zhan, *Electrochem. Commun.* 5 (2003) 903.
16. K.M. Ismail, Z.M. Khalifa, M.A. Azzem, W.A. Badawy, *Electrochim. Acta*, 47 (2002) 1867.
17. L. Zhao, W.K. Wang, A.B. Wang, Z.B. Yu, S. Chen, Y.S. Yang, *J. Electrochem. Soc.* 158 (2011) A991.
18. A.F. Christine, X.P. Shui, D.D. Chang, *J. Power Sources*, 41 (1996) 58.
19. B. Zhang, C. Lai, Z. Zhou, X.P. Gao, *Electrochim. Acta*, 54 (2009) 3708.
20. S. Komaba, T. Tanaka, T.Ozeki, T. Taki, H. Watanabe, H. Tachikawa, *J. Power Sources*, 195 (2010) 6212.